Iran University of Science and Technology

International Journal of

Railway Research

ISSN: 2423-3838

Crack Driving Force Calculation for a Railway Wheel Considering Thermoplastic Properties of the Wheel Material

Azade Haidari[1], Parisa Hosseini-Tehrani[1*]

[1]School of Railway Engineering, Iran University of Science and Technology, Tehran, Iran

ARTICLE INFO

Article history:
Received: 8.03.2020
Accepted: 24.05.2020
Published: 26.06.2020

Keywords:
Thermal load
J integral
EPFM
Crack
Railway wheel

A B S T R A C T

In this paper, the driving force calculation of a cracked railway wheel is studied, and the effects of thermal loads due to braking, train speed, and elastic-plastic material model are considered. Since the wheels are subject to fatigue loading and the property of its material is elastic-plastic, the study of crack growth in them is necessary because, in the case of existing a crack in the wheel and reaching its critical lengths, the failure of the wheel will occur. This is one of the important reasons for the accidents and derailment of trains. In this paper, the investigation of crack growth in the wheel is performed by two primary methods, linear elastic fracture mechanics (LEFM) and elastic-plastic fracture mechanics (EPFM) each of them has their specific condition of use. The applicability of each method in different conditions is discussed. The results demonstrate the importance of thermal loads of braking, train speed, and cyclic hardening material behavior on the usage of different approaches to achieve the appropriate crack driving force.

1. Introduction

Due to the elastic- plastic material property of a railway wheel and cyclic loading conditions, the fatigue and fracture of the wheels are one of the essential issues for the wheel manufacturers and their buyers. Wheels and axles are disassembled and checked for cracks in each major repair/rebuilding of the wagon. Having a crack on the wheel does not mean a complete rupture and sudden failure of the wheel. Therefore, it is necessary to have a criterion that can determine the remnant fracture life of the cracked wheel correctly and taking into account all the factors affecting the growth of the cracks. The absence of such a criterion results in the wheel being discarded before it reaches the end of its useful life. Considering the critical role that wheel safety plays in the safety of the train, it is necessary to review existing criteria for predicting crack growth and fatigue life of a cracked railway wheel and if it is needed, modified or expanded them so that it can cover all factors that affect the growth of cracks in the wheel in all ranges of elastic or plastic behavior of the wheel material. Today the lack of multiaxial fatigue and fracture life criterion for the cracked structures is observed [1]. In this paper, it is tried to provide an optimal range for the usage of the different criteria for estimating the growth of cracks in a railroad wheel. In this respect, some of the most related works for the growth of cracks, especially in the railway wheel, are mentioned.

Liu, Liu, and Mahadevan [2] examine models based on various critical planes and divide them into two groups of shear failure and tensile failure modes. Alizadeh, Ashofteh, and Asadi Lari studied the surface and subsurface cracks and concluded that increasing the contact force increases the possibility of nucleation and propagation of surface and subsurface cracks [3]. Based on their study, the plastic deformation and ductility of the wheel cause the creation of surface cracks. In every loading cycle, the plastic deformation in the contact area increases and cracks created and grown in mode II and III for

*Corresponding author, Associate professor
Email: Hosseini_t@iust.ac.ir

subsurface cracks. Also, thermal loads of braking cause normal crack propagation in the surface of the cracked wheels. Using the combination of low cycle fatigue (LCF) and ratcheting, the fatigue and fracture of rail and wheel can be predicted. Due to small plastic deformation in subsurface cracks, LEFM can be used for studying subsurface cracks, but in many existing studies, contact theory of Hertz is used for determining of contact forces, and rotation of the wheel on the rail was not modeled. Kwon, Lee, and Seo analyze the damage of the railway wheel with tread brakes. In their investigations, the cause of wheel treads damage was studied, and useful parameters such as contact stress and slop of wheels on the damage mechanism of the wheel were analyzed [4]. In many articles, the crack growth Studied in the wheel under bending moment using the Finite element (FE) model of rail and wheel. In their research, the crack growth behavior of the wheel after nucleation of the internal crack using the FE model and crack branching was studied by the 2D model. Kato et al. were calculating the rim stress below the tread surface of the wheel under rolling contact condition and showed that tensile residual stress due to rolling contact fatigue (RCF) increases at higher depths from the tread surface. They concluded that vertical cracks in the rim usually create at contact areas [5].

Based on Zucarelli et al. [6] studies on the railroad wheels, the temperature in the contact zone of rail-wheel does not reach to 300°c or higher, but on the condition of severe slipping or braking, due to higher temperature rise and quick cooling, the change in phase of wheel's material would occur. Kwon et al. Showed that interaction between brake blocks and tread surface of the wheel during the braking process, cause the generation of thermal crack on the tread surface of the wheel [7]. These thermal cracks for strong braking in high-speed trains are more critical. Peng et al. studies were predicting the crack growth in the wheel under mechanical loads, thermal loads of braking, and residual stress due to manufacturing using elastic-plastic FE analysis, but in their studies, the crack and brake blocks were not modeled [8]. Handa, Kimura, and Mishima focused on the thermal cracks on the tread surface of the wheel and indicated that these thermal cracks created under RCF and the cyclic frictional heat generated during the braking process. They studied the thermal cracks and their configuration experimentally [9]. Based on investigations, biaxially loaded structures are exposed to more martensite transformation while in shear loading conditions, the amount of martensite phase deformation is less and therefore for railway wheels which are in both axial and shear loading condition, the probability of creating martensite structures in severe braking is high but is not the subject of this article. The formation of martensite material on the wheel surface affected by the train speed, axle load, and braking power which is not considered in this paper and constant material properties for rail, wheel, and the axle is defined.

Peixoto and de Castro [10] modeled the crack propagation in the Spanish AVE railway wheel using the time-dependent stress of the wheel steel by testing the specimen under compact tension shear. The results of their research indicated that rolling contact loads induced mixed-mode conditions at the subsurface crack tip, which is far enough from the tread surface and its plastic deformation, therefore the LEFM could be used. Naderi studied the stress intensity factors (SIFs) in railroad wheels and investigated the crack length effect on crack growth. He showed that the simple 2D model for SIFs calculation using the finite element model is not applicable in the case that thermal loads of braking was applied and a 3D boundary element should be ued [11]. Liu and Gu [12] investigated the high-speed train and presented to have a safe trip, the wheel material should be improved by heat treatment, which causes an increase in strength and reduces the ductility. In their study, the crack on the rim of the wheel was analyzed. Based on their results, the thermal load of braking is the dominant force for crack propagation in the rim of the wheel. Investigations show that for a high-speed train, the material used in the manufacturing of the wheels has brittle behavior in wear condition, and therefore the growth of cracks in these wheels is of particular importance.

In 2017, Peixoto and de Castro considered three different load ratios and calculated the threshold of fatigue crack growth in a high-speed train. They found that the crack would turn to the direction which is perpendicular to maximum tensile load while the initial crack was perpendicular to the lower tensile load [10]. The wheelset of trains is under different static and dynamic loading conditions and therefore to prevent the sudden fracture of the cracked wheel

or axle, it is necessary to visit them in 20000000Km according to Dzugan et al. Studies [13]. They also investigated the fracture toughness of the wheel material for two different material Manufacturers the wheel.

Based on the performed studies there is a need for an appropriate criterion to investigate the growth of the crack with considering the combined mechanical and braking thermal loads, the effects of cyclic hardening, wheel speed, and occurrence of ratcheting.

In this paper, a cracked wheel with two brake shoes and a part of the rails are modeled, and the wheel rotation, the axial load on the wheel, the braking pressure applied during the braking process, and the increase in the temperature of the components due to braking are considered. Also, the cyclic hardening property of the wheel material and the effects of the plasticity around the crack are examined to provide an optimal range for the use of the proper criterion for estimating the growth of cracks in a railroad wheel in different conditions of usage.

2.FEA of Rail, Wheel and Brake Blocks

In this section, a finite element analysis (FEA) has been used to study a semi-elliptical edge crack at the wheel surface. At this stage, the wheel has an angular velocity of 50rad/s, and the axial load of 145KN is applied to the wheel center, and a reference point is defined at this point. Based on AAR standards, the axle load should be twice the nominal axial load in order to consider the dynamic load effects [14] in other words a quasi-static wheel load is usually multiplied by a dynamic factor of between 2 and 3. The reference point is coupled with the inner surface of the wheel. Two steps are considered in this modeling: rotation and braking. In the first step of the analysis, which is named the step of the rotation, only the wheel and rail contact is considered, and the brake shoes have not been added to the model. In the second step, that is the braking step, the brake blocks are added to the model and compressed to the tread surface of the wheel with a pressure of 400 MPa. Due to the relatively high friction coefficients in the contact areas, as well as the slip between the wheel and the rail, high normal and shear stresses creates in the contact zone, and partial slip occurs in these areas that may cause fracture.

The chosen element for mesh-making is a type of 8-node hexagonal element with linear interpolation (C3D8T). The tread surface of the wheel and the contact surface of the rail and brake blocks are meshed by 0.5mm element size, and for farther regions from the contact areas, the mesh dimensions become larger. The minimum and maximum mesh sizes used in the model are equal to 0.5-3mm according to mesh convergence analysis done for the model. The total elements used in the wheel are 45824.

During the braking process, localized hot bands or hot spots are created and expanded result in high-temperature, concentration, and high thermal stresses and strains creation. These hot spots have a much higher temperature than the points and areas around them and play a significant role in the nucleation and growth of fatigue cracks in the wheel surface and reduce the fractured life of the wheel. The angular variations in the surface temperature of the wheel are shown in Fig. 1. In this Figure, there are three peak areas, due to the wheel contact with the left-side brake block, the rail, and the right side brake block respectively. The points in the contact areas are heated by frictional heating until they are in the contact area and their temperature reaches a maximum local value and when leaving the contact area, these heated points are under the heat transfer through conduction to the rail and convection and are exposed to temperature drop

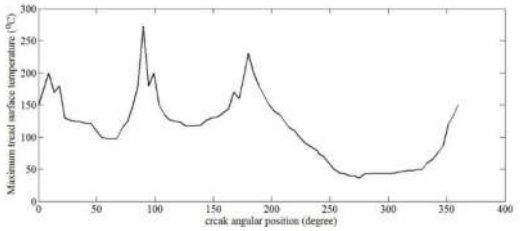

Figure1. The angular variations in the surface temperature of the wheel.

The equivalent stress intensity factor, which involves mixed-mode effects, is expressed by the following equation (2):

$$\Delta K_{mixed,eq} = \frac{1}{B}\sqrt{\Delta K_I{}^2 + (\frac{\Delta K_{II}}{s})^2 + (\frac{\Delta K_{III}}{s})^2 + A(\frac{\Delta K^H}{s})^2} \quad (1)$$

In this equation, the material parameter "s" is related to the material stress-strain, "A" and "B" are the material parameters and superscript "H" indicates the hydrostatic stress associated term.

These parameters and their values are explained by Liu et al.[2]

3. The Plasticity under Monotonic and Cyclic Loading

Plasticity is a critical issue in fracture mechanics because of the extent of plasticity and plastic deformation, in comparison to cracked specimen dimensions and crack size, determine the state of stress (plane strain or plane stress), and whether LEFM is applicable or not. If the size of the plastic zone is in the same order of crack length, LEFM is not valid for crack behavior study and due to the non-negligible effect of the plastic region around the crack, elastic-plastic fracture mechanics should be used which is discussed in the following. In a ductile material, there is a significant value of strain energy released by energy dissipation due to existing plastic deformation around the crack.

One of the most complex cases in the growth of the cracks is when the object is under cyclic loading. In this case, according to the Irwin model, the ideal plastic radius around the crack obtain by the following equation [16]:

$$C_{pc} = \frac{1}{3\pi}\left(\frac{\Delta K}{2S_Y}\right)^2 \quad (2)$$

An essential restriction to the use of LEFM is that the plastic zone size at the crack tip must be small relative to crack length as well as geometrical dimensions of the specimen. Under the monotonic loading condition, the plastic zone area (r_y) should be less than or equal to 1/8 crack length.

For the 145KN axle load, the ideal plastic radius under cyclic loading for a semi-elliptical crack with semi-minor and major axes of 5 and 7.5mm is equal to 0.3245e-6m for mechanical analysis and 0.550e-6m for thermo-mechanical analysis that is less than 1/8t and 1/8 (W-a). t is specimen thickness, a is the crack length and W is the width of the specimen. When the amount of plastic strains obtained from finite element results in the mechanical and thermomechanical analysis is smaller than ideal equivalent plastic deformation (PEEQ) , the radius of the monotonic plastic region is approximately zero, and therefore no back stress is created in the body, and the use of the stress intensity factors and J integral is suitable for investigating the crack behavior. For high plasticities which the back-stress region creates and continues until the end edge of the cracked object, using the conventional methods of LEFM and EPFM (the J integral presented by the Rice) is inefficient. In this case, it is necessary to use a relatively new method of configurational force calculation to determine the growth of the crack that is not the subject of this article.

The plastic zone (C_{pc}) around the crack for mechanical and thermo-mechanical analyses are

$$C_{pc,mechanical} = \frac{1}{3\pi}\left(\frac{\Delta K}{2S_Y}\right)^2 = \frac{1}{3\pi}\left(\frac{47.22}{2\times 450}\right)^2 = 3.245e-7,\ r_{tread} = 80mm \rightarrow$$

$$PEEQ_{mechanical} = \frac{C_{PC,mechanical}}{r_{tread}} = 0.4e-5 \quad (3)$$

$$C_{pc,thermomechanical} = \frac{1}{3\pi}\left(\frac{\Delta K}{2S_Y}\right)^2 = \frac{1}{3\pi}\left(\frac{61.5}{2\times 450}\right)^2 = 5.50e-7,\quad r_{tread} = 80mm \rightarrow$$

$$PEEQ_{thermomechanical} = \frac{C_{pc.thermomechanical}}{r_{tread}} = 0.6875e-5 \quad (4)$$

The values of equivalent plastic strain for the cracked wheel under 145KN are shown in Fig. 2. As can be seen from this Figure, the values of plasticity for both mechanical and thermomechanical analyses are less than the ideal mechanical and thermo-mechanical C_{pc}, and therefore LEFM can be used for studying the crack growth in railway wheel for 50rad/s velocity and 145KN axle load.

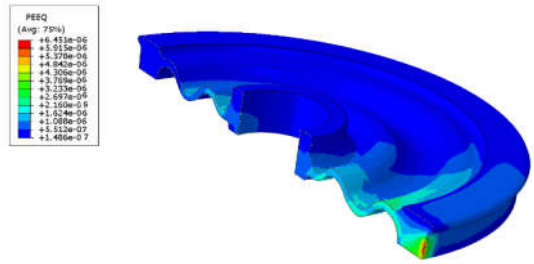

(a)

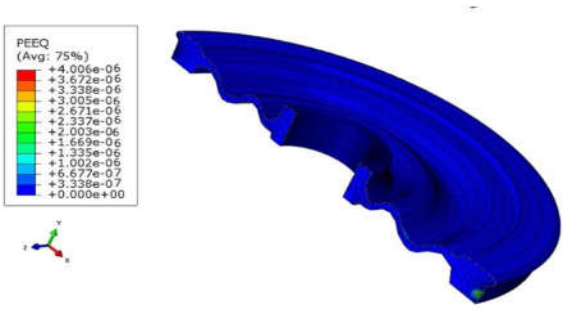

(b)

Figure 2. The equivalent plastic strain of the wheel under 145KN axle load for a) mechanical analysis and b) thermo-mechanical analysis.

Hence, the Abaqus output is used to obtain stress intensity factors and the maximum strain energy density method for estimating the direction and plate of the crack growth.

Stress intensity factors are obtained using the displacement discontinuity method by equations presented by Sheibani et al. [15]. Based on FEM, for the first increment of crack growth, θ_0 has small values (for mechanical analysis $\theta_0 \sim 11^o$ [the initial crack position is perpendicular to the rail-wheel contact plate] and for thermo-mechanical analysis $\theta_0 \sim 0^o$). Over time and with further crack increment, the value of θ_0 reaches to 65^O for mechanical analysis and 75^O for thermo-mechanical analysis in the last increment of crack growth, which according to the results mentioned by Meizoso, et al. [1] (1991), shows good agreement with reality. In Fig. 3 variations of crack direction during crack growth is shown

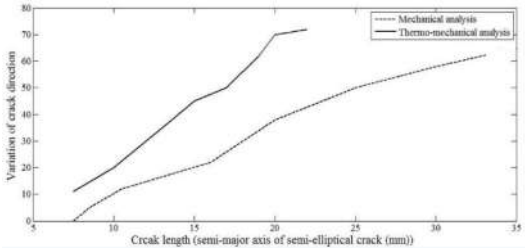

Figure 3. Crack growth direction and critical crack length.

The horizontal axis in Fig. 3 represents the final length of the semi-major axis of the crack, which, as can be seen, its amount for thermo-mechanical analysis is considerably less than its corresponding value in the mechanical analysis (the critical crack length is 23mm in thermo-mechanical analysis and 33mm in the mechanical analysis). These critical lengths are equal to the length of the semi-major axis of the crack where $K_{IC} \leq Keq$.

Based on the results obtained here, as well as the results in Martin Meizoso et al. study, at the beginning of crack growth, K_I dominates all other components of the stress intensity factors and, the initial growth of the crack occurs almost in its initial plate. The effect of shear stresses (σxz, σyz) and their related stress intensity factors (K_{II}, K_{III}) has increased with the increasing crack growth and in higher increments of crack length. According to empirical observations, the final crack is created outside the initial crack plane at an angle of $\theta 0 \sim 80^o$ [1].

The following equation may be used to estimate the crack growth life [2].

$$N(a) = \frac{1}{C(\Delta F)^m} \int_{a_0}^{a_c} \frac{(1-R)^{\zeta m} da}{\sqrt{\pi a} Y(a)^m} \quad (5)$$

The parameters of the equation above are expressed by (Liu, Liu, and Mahadevan 2007). The fracture life of the wheel under mechanical loads, estimated to be 1.2×10^6 cycles approximately, which corresponds well to the results by Kwon et al. [17] while in thermo-mechanical analysis, the fracture life drops to 0.7×10^6 cycles.

The semi-minor diameter of the crack obtained in mechanical and thermo-mechanical analyses is 18 mm and 10 mm, respectively. Therefore, it can be concluded that the critical crack dimensions of the thermo-mechanical analysis are less than the mechanical analysis, which is one of the reasons for less fatigue life in thermo-mechanical analysis versus mechanical analysis. The critical crack size is equal to the length of the semi-minor and major diameters of the crack at the moment that K_{eq} value reaches the amount of fracture toughness (K_{IC}). The approximate value of the semi-major axis of crack obtained 32-33mm from mechanical analysis, and it matches the value obtained by Kwon et al. [17].

After ensuring the accuracy of the model by comparing the results in this paper with experimental observations and existing research, at this stage, the axial load will be increased to 200 KN and, we will consider the problem-solving method. In this case, the J integral method is used due to the irrefutable plasticity around the tip of the crack.

4. J integral calculation in 200KN axle load

By increasing the axial load and strain of the body which causes the formation of larger plastic deformation on the wheel, the LEFM does not give the correct results, and the elastic-plastic fracture mechanics approach (J integral method) must be used. The following Figure shows the plastic region around the crack for a semi-elliptical surface crack with the axial load of 200 KN and 50rad/s angular velocity

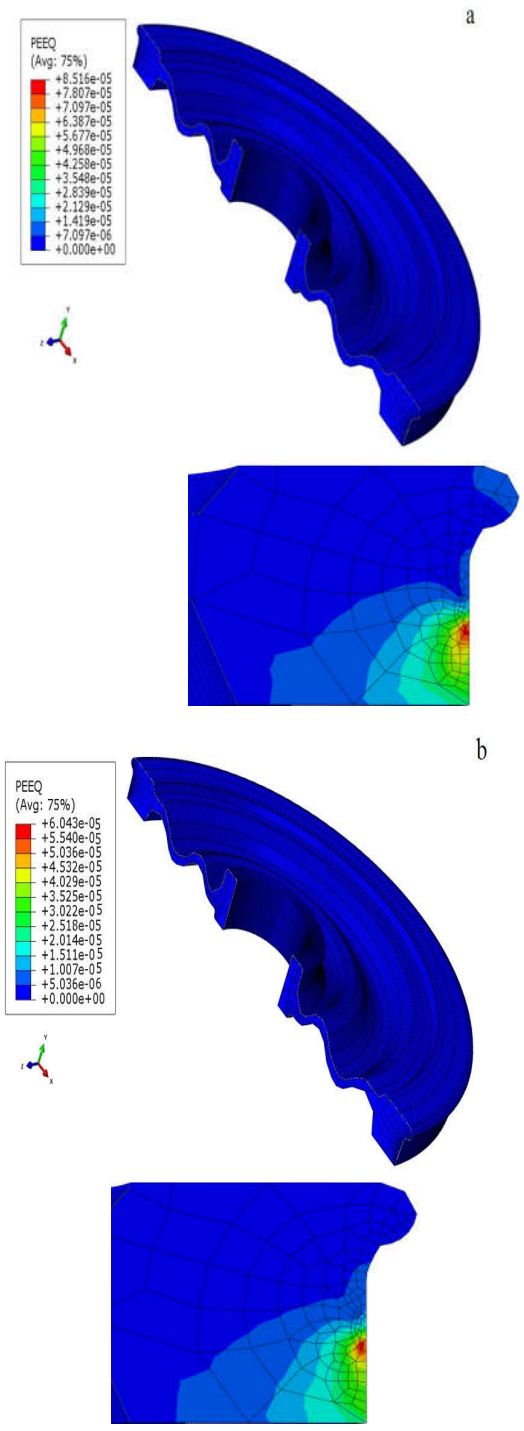

Figure 4. PEEQ contour of railway wheel under axle load of 200KN for a)thermo-mechanical loading and b)mechanical loading.

As can be seen from Fig. 4, the maximum value of equivalent plastic strain considering 200KN axle load is 6.043e-5 and 8.516e-5 for mechanical and thermo-mechanical analysis, respectively. These amounts are more significant than corresponding C_{pc} and therefore using the LEFM for 200KN axle load is not a proper method. In this case, the energy method based on J integral should be applied.

In this section, the traditional J-integral method (J_{nlel}) is used. It is possible to obtain J integral values for different contours around the crack tip using the direct outputs of the Abaqus for elastic-plastic materials in the contained yielding region. In Table 1, the values of the J integral obtained from the output of Abaqus (J_{nlel}) for several contours around the crack tip in mechanical and thermo-mechanical analyses are shown.

Table 1. J integral values in mechanical and thermo-mechanical analysis for ω=50rad/s and 145KN axle load.

	Γ_{tip}	Γ_1	Γ_7	Γ_8	Γ_9	Γ_{far}
Mechanical J^{nlel}	135.38e3	154.9e3	896e3	902.67e3	917.23e3	920e3
Thermo-mechanical J^{nlel}	249.92e3	261.2e3	1232e3	1254.4e3	1273e3	1280e3

As can be deduced from Table 1, the difference between mechanical and thermo-mechanical values in each contour is significant, which indicates the importance of thermal loads of braking. For example, for the first contour considered in the surroundings of the crack tip, the difference between mechanical and thermo-mechanical values is 68.6%, which is a significant difference.

Due to the importance of the thermal loads and strains generated by the brakes, it is necessary to consider correction terms for finding the thermal effects of braking. The second integral in (6) shows the effect of thermal strain created in the braking process on the value of thermo-mechanical J integral.

$$J_F^* = \int \left(W\widehat{n_\beta} - \widehat{T_i}\widehat{u_{i;\beta}}\right)d\Gamma + \int \left\{\widehat{\sigma_{ij}}\widehat{\varepsilon_{ij;\beta}^{th}}\right\} dA \qquad (6)$$

In (6) W, n_β, T, and u represent the strain energy density, the unique vector perpendicular to the contour, stress, and displacement vectors respectively. ";" Represents derivative operations and ε^{th} is the thermal strain created during braking

The J integral values obtained from the finite element analysis of the wheel, rails, and brake shoes for the ten contours considered in the model are shown in Fig. 5. The Abaqus software takes the number of contours necessary to calculate the J integral. The first contour is a ring

of elements that immediately lies in the vicinity of the crack tip, and the farther contours are created by moving away from the boundaries of the cracks. Since the J integral must be independent of the path, variations can be seen along the first contours, but for contours that are sufficiently far from the tip of the crack and its surrounding plastic region, the answers must converge. Based on the FE results of this article, from contour 9 and 10, the condition of path independency of the J integral is satisfied (as shown in Fig. 5).

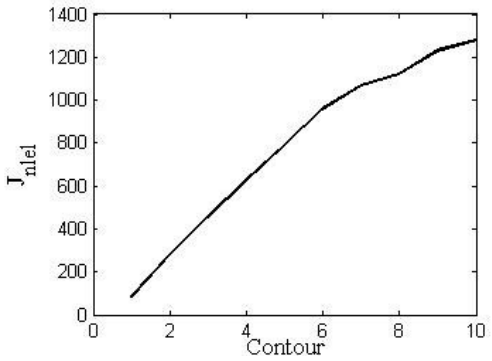

Figure 5. J integral obtained from the output of Abaqus for thermo-mechanical analysis.

The finite element results for a wheel are shown in ten contours around the crack. As can be deduced from the above Figure, the results obtained from the contours seven to ten are closer, while the results show fluctuating for the contours close to the boundaries of the crack. The gradient of the graph for the contours closer to the tip of the crack is more considerable and, the convergence rate for these inner contours is less. Based on the Abaqus benchmark manual, the calculation of J integral in these contours (internal contours) cannot be considered due to the instability of the stresses and plastic strains in the crack. Also, the stability and convergence of the results obtained from the contours sufficiently far from the tip of the crack (outer contours) represent the acceptable component meshing.

4.1. Thermal strain effect on the non-linear J integral

To obtain the effect of thermal strain on the J integral value for semi-elliptical crack considered in this study, the analyses are performed once with considering the thermal loads of braking (thermo-mechanical analysis) and once again without considering these thermal loads (mechanical analysis). Therefore, by comparing the difference in the results of the two analyses, we can find the role of the thermal loads and thermal strains on the value of J integral.

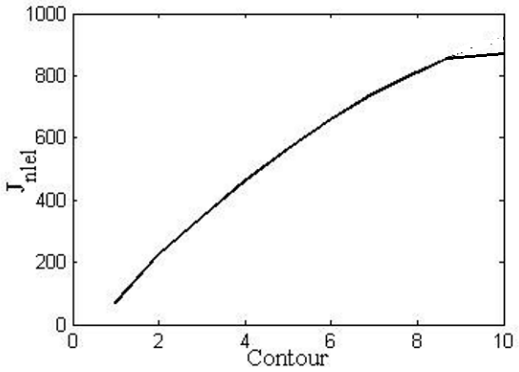

Figure 6. J integral values in the mechanical analysis.

In Fig. 6, the mechanical J integral for ten contours around the crack front at the end of the braking step is illustrated. As can be seen from this Figure, The convergence rate of the J integral value increases with the increasing number of contours, and the slope of the curve for the farther contours from the crack tip decreases.

4.2. Effects of speed on driving force

By increasing the velocity of the wheels, the amount of heat generated during braking in contact zones increases, according to Eq. (7). Therefore, thermal stresses and strains become higher, and the area of plastic deformation expanded and higher plastic strains created around the crack tip, and as a result, the crack driving force increases.

$$q = \frac{\mu NV}{A} \tag{7}$$

In this equation, μ is the friction coefficient in contact pairs, N is the normal force in contact plane, V is velocity, and A is the contact area. In this section, the PEEQ for an axle load of 200KN and angular velocity of 100rad/s in both mechanical and thermo-mechanical analyses are shown.

In the following table, the values of J integral in mechanical and thermo-mechanical analyses are shown. Comparing the results of table 1 and table indicates by increasing the speed, the values of J integrals increase too, and due to higher plastic deformation created by increasing

the velocity, the rate of J integral convergence decreases as can be seen in Fig. 8.

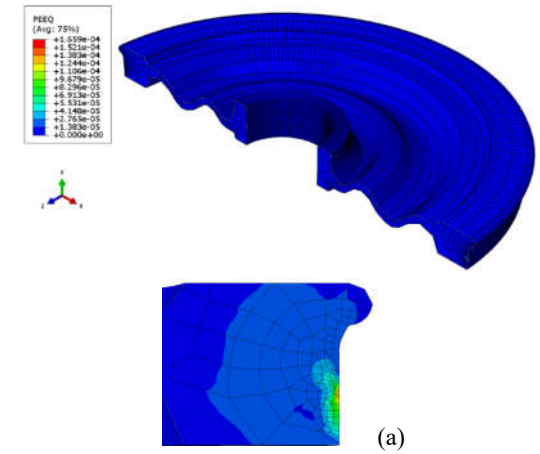

(a)

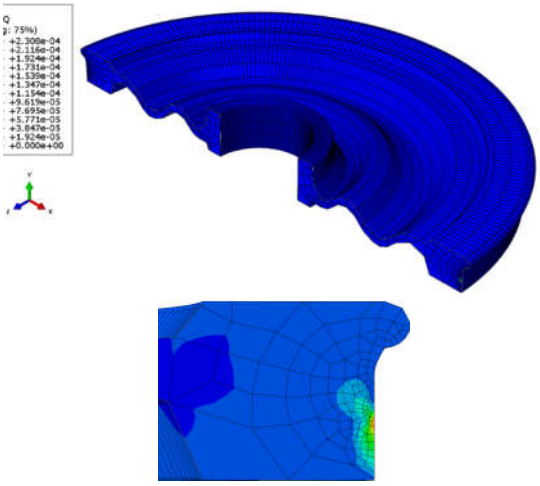

Figure 7. PEEQ for ω=100rad/s and 145KN a) mechanical analysis and b) thermo-mechanical analysis.

Table 2. J integral values in mechanical and thermo-mechanical analysis for ω=50rad/s and 200 axle load.

	Γ_{tip}	Γ_1	Γ_7	Γ_8	Γ_9	Γ_{far}
Mechanical J^{nlel}	263e3	584e3	1281e3	1380.7e3	1446.2e3	1528e3
Thermo-mechanical J^{nlel}	460e3	934.4e3	2049e3	2190e3	2300e3	2380.2e3

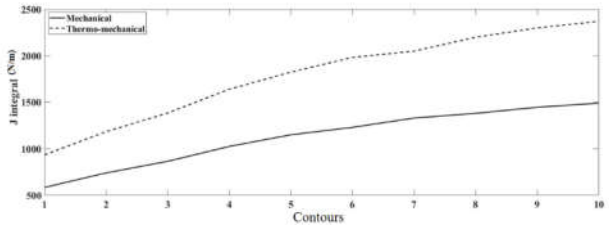

Figure 8. Variation of plastic strain around the crack tip for different contours.

4.3. Plastic strain accumulation due to Kinematic hardening (ratcheting behavior) of the wheel

Generally, the material response to cyclic loading can be divided into 4 different states: elastic, elastic shakedown, plastic shakedown, and ratcheting. If the cyclic stress is lower than the elastic shakedown, the material response after several cycles reaches to elastic shakedown and the fracture occurs in high cycle fatigue. But in the case that the cyclic stress is higher than elastic shakedown, the material doesn't show the elastic shakedown behavior and in each cycle, the plastic deformation creates and fracture happens in low cycle fatigue. The closed-loop of stress-strain only exists under plastic shakedown and if the loop was open, in each loading cycle the plastic strain changes and accumulates and this phenomenon called ratcheting.

According to Fig. 9 and Table 3, the equivalent stress created in the wheel under 200KN axle load is much higher than the maximum plastic stress in Table 3 (958.125MPa). Therefore the material exceeded the shakedown limit and due to changing the plastic deformation in each cycle (as shown in Fig. 10), the material shows the ratcheting behavior, and plastic deformation accumulates in each load cycle.

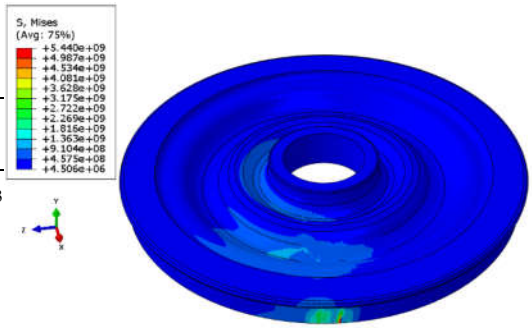

Figure 9. Von Mises stress contour of the wheel in 200KN axle load.

Table 3. Stress and strain values for the isotropic hardening material of the wheel.

Plastic stress (MPa)	Plastic strain
545	0
763.625	0.02099
887.25	0.0445
958.125	0.0863

The isotropic hardening model is considered in Abaqus software in accordance with the numbers in Table 3. As can be seen from Fig. 10, the plastic strain increase in each load cycle for both isotropic and non-linear kinematic model and the maximum strain in both isotropic and non-linear kinematic model is higher than the shakedown limit (0.0863 in Table 3) and this cause accumulation of plastic deformation known as ratcheting phenomenon. On the other hand, the values of plastic strains in the kinematic model are considerably more than the isotropic model and therefore, the plastic strain accumulation in non-linear kinematic properties is dominant and is referred to ratcheting.

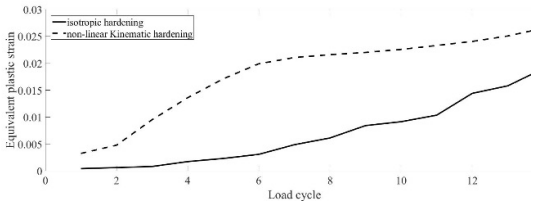

Figure 10. The variation and accumulation of plastic strains during each load cycle.

According to empirical observations [3, 6] rolling and slip between the wheels-rails and brake blocks-when exceeded from the shakedown limit and the plastic strain accumulation occurs near the surface layers during each loading cycle. To analyze and simulate this process, it is necessary to use the cyclic Kinematic hardening law, which plays an essential role in the failure of the wheel. Most of the previous analyses were based on the fact that the material is ideally elastic or completely plastic and without any hardening. The idea of an ideal plastic material mainly estimates the plastic strain more than reality. The ratcheting (accumulation of plastic strains) is an inevitable phenomenon occurring in the railway wheel under cyclic hardening properties. In this part of the study, the premise of the elastic-plastic material under cyclic loading is examined. In this situation, the plastic deformations are accumulated in each cycle. Due to wheel rotation and the effects of non-vanishing of plasticity caused by the kinematic and isotropic hardening assumption, J integral value considering the plasticities of cyclic hardening should be calculated. The nonlinear kinematic hardening model is used in this section in Abaqus software, and the obtained results are compared with the isotropic hardening model. The used ratcheting model consists of two components of non-linear kinematic and isotropic hardening.

In Table 4 the values of J integral for elastic shakedown model and the ratcheting model for mechanical and thermo-mechanical analyses are illustrated.

Table 4. Variation of J integral for different contours in hardening and elastic material property for ω=100rad/s and 200KN axle load.

	Γ_{tip}	Γ_1	Γ_2	Γ_7	Γ_8	Γ_9	Γ_{far}
$J_{elastic}^{Mechanica}$	263e3	584e3	960e	128 1e3	138 0e3	144 6e3	152 8e3
$J_{ratchettin}^{Mechanica}$	388e3	724e3	128 0e3	158 0e3	161 0e3	175 4e3	186 0e3
$J_{elastic}^{thermo-m}$	460e3	934. 4e3	162 9e3	204 9e3	219 0e3	230 0e3	238 0e3
$J_{ratchettin}^{thermo-m}$	569e3	123 0e3	196 4e3	139 4e3	248 0e3	264 5e3	267 3e3

Comparison of the data of Table 4 obtained for elastic-plastic material under isotropic hardening and ratcheting of the wheel in two analyses of the mechanical and thermo-mechanical show the importance of kinematic hardening effect in reducing the fracture life of the railway wheel.

5. Conclusions

Based on the plastic zone size of the cracked wheel obtained from FE results, the choice of a suitable criterion for studying crack behavior is necessary. In this study, the effects of some parameters such as thermal loads due to braking and ratcheting on the results have been indicated as follows;

1-The effect of thermal stresses created during braking on stress and strain fields created in the wheel is very significant so that the degree of thermal stress and mechanical stresses are the same and cannot be ignored. Hence, to have a more precise analysis, it is necessary to consider the thermal loads of braking by modeling the brake blocks and braking pressure. The difference between the fracture life of the wheel under 145KN axle load for two mechanical and thermo-mechanical analysis is 71%, which is non-negligible.

2- Modeling the rails and brake blocks improve the accuracy of the results because they can be used to measure the applied pressure and dimensions of the contact areas as well as the local hot spots created at the contact points in the analyses. If the brake shoes are not modeled, it is impossible to consider the contact pressure and the local heat generated at the wheel surface in the contact zone between the wheel and brake shoes, which reduces the accuracy of the results. Based on observations, in the wheel contact regions with rails and brake shoes, hot spots are localized and result in higher local thermal stresses (45% higher than mechanical stress), that if be ignored lead to an over-estimated lifetime (71 % greater than actual life) and dramatically reduces design security.

3- The results show by increasing the train speed (angular velocity of the wheels) the number of rolling contact between rail-wheel increases and therefore, the mechanical stresses and strains increase too. On the other hand, according to equation 7, the heat generated in contact areas has a direct relation with the velocity of the wheel and as a result, the thermal loads and thermal stresses and strains get more prominent and therefore the values of J integral and driving force for both mechanical and thermo-mechanical analysis increase which cause reduction the fracture life of the cracked wheel.

4- The role of non-linear Kinematic and isotropic hardening of the wheel on the growth of the cracks is another parameter studied in this article. The results show that by considering the hardening properties, plastic deformations increase and accumulate and the size of the plastic area around the cracks increases, and ratcheting will occur which may change the problem-solving method from LEFM to EPFM. The difference between the results of the isotropic hardening properties (Table 3) and ratcheting model (considering the non- linear kinematic hardening) model, is due to the more accumulation of plastic strains and deformations in each cycle in the non-linear kinematic model in comparison with the isotropic model.

References

[1] A. Martín Meizoso, J. M. Martínez Esnaola & M. Fuentes Pérez, Approximate crack growth estimate of railway wheel influenced by normal and shear action, Theoretical and Applied Fracture Mechanics, 15 (1991), 179-190.

[2] Y. Liu, L. Liu & S. Mahadevan, Analysis of subsurface crack propagation under rolling contact loading in railroad wheels using FEM, Engineering Fracture Mechanics, 74 (2007), 2659–2674.

[3] J. Alizadeh K., R. S. Ashofteh, A. Asadi Lari, Numerical Analysis of Fractured Process in Locomotive Steel Wheels, International Journal of Mechanical and Mechatronics Engineering, 7 (2013) 479-483.

[4] S.J.Kwon, D.H.Lee, J. W.Seo, H.K. Jun & J. ChulKim, Failure Analysis for Power car Wheels based on Contact Positions and Tread Slope, Engineering Failure Analysis, 80 (2017), 1-10.

[5] T. Kato, T. Makino & K. Hirakawa, The effect of slip ratio on the rolling contact fatigue property of railway wheel steel, International Journal of Fatigue 36(2012), 68–79.

[6] T.A. Zucarelli, M. A. Vieira, L. A. Moreira Filho, D. A. P. Reis & L. Reis, Failure analysis in railway wheels, Procedia Structural Integrity, 1 (2016), 212–217.

[7] S. J. Kwon, J.W. Seo, H. K.Jun & D.H. Lee , Damage evaluation regarding to contact zones of high-speed train wheel subjected to thermal fatigue, Engineering Failure Analysis, 55 (2015), 327-342.

[8] D. Peng , R. Jones Ac, T. Constable b & S. N. Lingamanaik, The tool for assessing the damage tolerance of railway wheel under service conditions, Journal of Theoretical and Applied Fracture Mechanics, 57 (2012), 1–13.

[9] K. Handa, Y. Kimura & Y. Mishima, Surface cracks initiation on carbon steel railway wheels under concurrent load of continuous rolling contact and cyclic frictional heat, Wear, 268 (2010), 50–58.

[10] D. F. C. Peixoto, P. M.S.T. de Castro, Mixed mode fatigue crack propagation in a railway wheel steel, Procedia Structural Integrity 1 (2016), 150–157

[11] A. Naderi, Numerical investigation on stress intensity factor in railway wheelset under the influence of residual stresses induced by press fitting process, Engineering Failure Analysis, 94 (2018), 78-86.

[12] Z. X. Liu & H. C. Gu, Failure Modes and Materials Performance of Railway Wheels, *Journal of Materials Engineering and Performance*, 9 (2000), 580-584.

[13] J. Dzugan, Y. Ito, S. Kwon, K. Ogawa & T Shoji, Fracture toughness tests of wheelset materials used in the Japanese Shinkansen express trains, Proc. Instn Mech. Engrs Part L: J. Materials: Design and Applications, 218 (2004), 263-271.

[14] L. Ramanan, R. Krishna Kumar &, R. Sriraman, Thermo-mechanical finite element analysis of a rail wheel, International journal of mechanical science, 41(1999), 487-505.

[15] F. Sheibani & J. E. Olson , Stress Intensity Factor Determination for Three-Dimensional Crack Using the Displacement Discontinuity Method with Applications to Hydraulic Fracture Height Growth and Non-Planar Propagation Paths, ISRM International Conference for Effective and Sustainable Hydraulic Fracturing, At Brisbane, Australia

[16] R. Hosseini, R. Seif, Influence of Hardening on the Cyclic Plastic Zone Around Crack Tip in Pure Copper CT Specimens, Journal of Stress Analysis, 2 (2017), 43-53.

[17] S. J. Kwon , D. Hyung Lee, J. W. Seo & S. T. Kwon, Safety margin evaluation of railway wheels based on fracture scenario, International journal of railway, 5 (2012), 84-88.